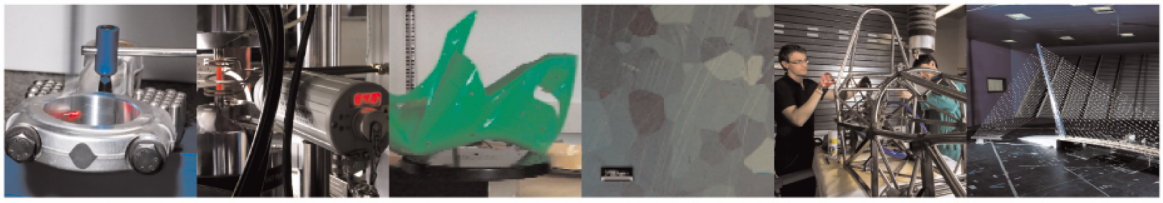

Wind tunnel tests on railway vehicles in the presence of windbreaks: Influence of flow and geometric parameters on aerodynamic coefficients

Brambilla E.;Giappino S.;Tomasini G.

This is a post-peer-review, pre-copyedit version of an article published in Journal of Wind Engineering and Industrial Aerodynamics. The final authenticated version is available online at: https://doi.org/10.1016/j.jweia.2021.104838

DIPARTIMENTO DI MECCANICA ■ POLITECNICO DI MILANO
via G. La Masa, 1 ■ 20156 Milano ■ EMAIL (PEC): pecmecc@cert.polimi.it
http://www.mecc.polimi.it
Rev. 0

Title page

Article title: Wind tunnel tests on railway vehicles in the presence of windbreaks: influence of flow and geometric parameters on aerodynamic coefficients

Author names and affiliations; Brambilla Elia[1], Stefano Giappino[2], Gisella Tomasini[1]
[1]Department of Mechanical Engineering, Politecnico di Milano, via La Masa 34, I-20156, Milano, Italy
[2] Galleria del vento Politecnico di Milano (GVPM), via La Masa 34, I-20156, Milano, Italy

Corresponding author: Brambilla Elia elia.brambilla@polimi.it

Wind tunnel tests on railway vehicles in the presence of windbreaks: influence of flow and geometric parameters on aerodynamic coefficients

E. Brambilla[1], S. Giappino, G. Tomasini[1]

[1]Department of Mechanical Engineering, Politecnico di Milano, via La Masa 34, I-20156, Milano, Italy
[2]Galleria del vento Politecnico di Milano (GVPM), via La Masa 34, I-20156, Milano, Italy
Corresponding author: E. Brambilla, elia.brambilla@polimi.it

Abstract

Crosswind stability is one of the most studied topics in the field of train aerodynamics. The interaction between a train and strong crosswinds can lead to the train overturning. One way to reduce the train overturning risk is to equip the railway line with windbreak barriers. In this work, the results obtained during wind tunnel tests on an ETR1000 high-speed train in the presence of different types of windbreaks are shown. The goal is to underline the effects of different flow parameters and geometric parameters of the infrastructure's models on the train's aerodynamic coefficients. Comparing the different test results made it possible to provide indications on which parameters are important to avoid experimental errors and reproduce as much as possible the real full-scale phenomena. Particular attention shall be paid to the dimensions of the splitter plate because a limited upwind width can lead to underestimation of aerodynamic coefficients by more than 30%. The length of the barriers in front of the train is fundamental and too short length can lead to coefficients overestimation of about 25%. Finally, coefficients measured with only the upwind windbreak row are lower (up to 50%) than those measured with a two rows configuration.

Keywords: railway vehicles, wind tunnel tests, crosswind, windbreaks, wind fences.

1 Introduction

In the early years of railway development, the main aerodynamic problem considered was aerodynamic drag [1]. However, with the advent of high-speed trains, new issues arose and became constraints for railway network builders and operators.
The aerodynamic phenomena involving a train have different characteristics depending on whether the train runs in the open air or in confined spaces, such as railway tunnels.
In the open air, an important role is played by the atmospheric wind that may come from different directions in relation to the train's direction, called crosswind [2]. To this aspect gives rise to a safety risk of the train overturning in strong crosswind conditions. In Europe, within the framework of the Technical Specification for Interoperability (TSI) [3] and in European standard EN14067-6 [4], the evaluation of the train safety in the presence of crosswind is mandatory for high-speed trains.
The risk assessment procedure coded in EN14067-6 involves the determination of the train's aerodynamic coefficients, the development of the train's dynamics model and the calculation of the Characteristic Wind Curves (CWCs). Depending on the train type, small differences in the procedure are allowed.
For high-speed trains, wind tunnel tests are mandatory for calculating the aerodynamic coefficients and many constraints on flow parameters (Reynolds number, ABL profile, turbulence intensity, etc.) are established, in order to make the wind tunnel test results consistent and representative of the full-scale conditions.
European standard EN14067-6 is the result of several studies that were performed over the last 20 years to better understand the crosswind phenomenon and to develop methodologies able to

evaluate the level of safety of a rail vehicle in terms of overturning risk. To face the problem, various countermeasures have been adopted by train manufacturers and infrastructure managers: optimization of train shapes [5], regulation of train operation (i.e. limitation of the train's speed) and construction of windbreak facilities [6].

Windbreaks have been proven to be an efficient and practical solution for mitigating crosswind effects. In the last 10 years, their performance has been investigated by various authors, mainly by means of wind tunnel tests and CFD simulations.

Thanks to the possibility of adopting moving meshes, CFD analyses are carried out by correctly reproducing the relative movement between the train and windbreaks, simulating the real boundary conditions. The main target of these studies with moving meshes is to evaluate the effects of geometric irregularities or gaps in the windbreak array [7] [8] [9] [10] [11]. Anyway, as also underlined by Hashmi et al. [12], most of these CFD studies lack accurate validation data measured from experimental tests.

On the other hand, tests in wind tunnel, both in the presence of windbreaks or other scenarios (embankment, viaduct, flat ground or single/double track), are carried out mainly with static train models and fixed ground, with the exception of only few cases ([6],[13],[14]).

These tests were performed in recent years to validate CFD studies (at least with static ground and train models, [15], [16]) or to study the effects of different types of barriers/geometrical configurations (height, distance from the rail, inclination, etc.) on aerodynamic force coefficients.

Among the most recent works, wind tunnel tests with stationary ETR500 train model placed near different windbreaks were performed by Tomasini et al [17]. It was shown that the 40% porous barriers tested significantly reduce the rolling moment coefficient by more than 30% at all absolute wind angles. In addition, the presence of the barriers considerably reduces the sensitivity of all force/moment coefficients to the Reynolds number.

Hashmi et al. [12] measured the surface pressures acting on a stationary Class 390 Pendolino train in a wind tunnel, with different wind angles and different windbreaks. The work also considers geometrical changes to the distance between the train and the windbreaks. For the tested scenarios, differences in terms of pressure distributions on the train's surface and overall mean aerodynamic load coefficients, are shown.

In general, wind tunnel tests on static train models with windbreaks present two macro-issues:

1. The capability of the static tests to represent the real conditions, considering that the relative train / windbreak motion is not correctly reproduced.
2. The flow (turbulence intensity, Re number, etc.) and geometrical parameters to be respected in the wind tunnel tests to get these tests free from experimental errors and consistent with full-scale conditions.

About the first item, for the case without windbreaks, there are a lot of papers that have demonstrated the validity of static wind tunnel tests [13] [18] [20].

When the windbreaks are added to the scenario, the relative motion between the train and the barriers is null and this means that, unlike the real case, the relative wind / train and wind / barriers velocities are equal.

Anyway, even if some authors in the past questioned the validity of static wind tunnel tests with barriers [12], by observing that a windbreak wall creates a greater number of large vortices around the train which are affected by the train's motion [18], more recent studies have demonstrated that static wind tunnel tests with porous barriers are able to correctly reproduce the real situation, in this condition as well [20]. In this work, static wind tunnel tests with windbreaks were used to validate a moving mesh CFD model, which instead reproduce the real operative conditions. Comparing CFD results and wind tunnel measurements for relative flow yaw angle of 20°, the train aerodynamic coefficients result very similar both cases. The equivalence of static wind tunnel tests with windbreaks and the real situation must be considered valid only for the type of barriers and train under investigation in [20] and it is not possible to affirm a priori that the same equivalence is also valid for other train/barrier configurations (this point will be discussed in another paper). The key

point is that it was possible achieve this conclusion thanks to wind tunnel tests, which allowed to validate the CFD numerical models.
Thus, considering that static wind tunnel tests represent a simplification of a more complex engineering problem, but that they are useful for getting an initial evaluation of the performance of porous barriers and can be used to validate CFD simulations, the second issue, that is, which are the correct flow and geometrical parameters to be simulated to make these tests free from experimental errors and as consistent as possible to real conditions, needs to be solved.
The current version of European Regulation EN14067-6 does not indicate any procedure for evaluating train safety in the presence of windbreaks.
The aim of this work is to give some guidelines about the effects of the main flow and geometrical parameters on the aerodynamic coefficients measured in static wind tunnel tests with windbreaks. In particular, the sensitivity of the aerodynamic load to the following parameters is considered:

- Re number.
- Turbulence intensity.
- Incoming boundary layer.
- Splitter plate width.
- Length of the windbreak arrays.
- Presence of upwind and downwind rows in the windbreak array.

In order to understand the physical reasons associated with a variation in the parameters studied, not only force but also pressure coefficients are measured and thanks to the pressure distribution the modification induced in the flow around the vehicle is inferred.

2 Experimental setup

2.1 Wind tunnel facility and flow characteristics

Experimental tests are performed in the Politecnico di Milano Wind Tunnel (GVPM). GVPM is a closed-circuit facility arranged vertically. The main feature of this facility is the presence of two test sections with very different characteristics, offering a very wide spectrum of flow conditions, from very low turbulence and high-speed in the contracted section, to earth boundary layer simulation in the large wind engineering test section. The overall wind tunnel characteristics are summarized in Table 1.

Table 1: GVPM wind tunnel characteristics.

GVPM: Politecnico di Milano Wind Tunnel			
Test Section	**Size (width, height, length) [m]**	**Max Speed [m/s]**	**Turbulence Intensity [%]**
Low-speed	13.84, 3.84, 36	16	2
High-speed	4, 3.84, 6	55	0.15

The high-speed test section is 4 m wide, 3.84 m high and 6 m long. It is possible to carry out both closed chamber and free jet tests. The maximum achievable speed is 55 m/s, with a turbulence level of 0.15%. For these specific tests, the test section is equipped with a splitter plate 0.5 m high (to control the

boundary layer) with a rotating central part (Diameter=2.5 m) on which the train models and the scenario (ballast, track and windbreaks) are fixed, in order to change the flow's angle of attack in relation to the model.

The boundary layer test section is 13.84 m wide, 3.84 m high and is specifically designed for wind engineering tests on scale models of civil structures. The maximum wind speed is 16 m/s and the turbulence index in "smooth flow" conditions (without the addition of turbulators) is about 2%. The constant section chamber, 35 m long, allows the installation of active or passive turbulence generators, in order to simulate the atmospheric boundary layer with a turbulence intensity that can be higher than 35%.

Also in this test section, the model and the scenario are fixed to the supporting table, in order to meet the requirements related to the air speed profile. Then, the supporting table is installed on a 13 m diameter rotating platform.

The free stream velocity is measured in both test sections.

In high-speed test section the mean flow velocity is evaluated by measuring the static differential pressure in two points of the wind tunnel convergent, while in low-speed test section, the mean velocity is measured by a pitot tube placed about 6 m upwind with respect to the model at 0.5 m from the floor of the test section.

Tests with windbreaks were carried out in both test sections.

Considering the characteristics of each test section, in the high-speed test section it is possible to evaluate the effect of the Reynolds number in the presence of windbreaks.

In the low-speed test section, thanks to its larger size, it is possible to evaluate the effect of different lengths of the barriers in front of the train and of different splitter plates.

Furthermore, comparing the results of the two test sections will give indications on the effect of the height of the boundary layer and the turbulence intensity.

According to European Regulation EN14067 [5], the air flow simulated in the wind tunnel must comply with specific constraints.

Table 2 summarises the parameters regulated by the EN standard, the limit values and the corresponding values measured in the two test sections.

Parameter D (shown in Figure 1) is the distance between the front of the vehicle model and the front end of the scenario. Another geometric parameter is the ratio between the total length of the train model (leading + trailing vehicles = L_{Train}) and the wind tunnel width (L_w). According to the EN standard, the distance D should be more than 8 m full-scale and the ratio L_{Train}/L_w should be lower than 0.75.

The thickness of the boundary layer ($\delta_{99\%}$) at the axis of rotation of the instrument-fitted model on the splitter plate in the high-speed test section is equal to about 40 mm, which corresponds to about 15% of the height of the vehicle (well below the regulatory requirement of 30%) while in the boundary layer test section it is about 80 mm, higher than in the other section but still compliant with the standard requirement.

Other constraints concern the maximum turbulence intensity (Iu) and the minimum Reynolds number (Re), calculated using a train characteristic dimension of 3 m in full-scale.

The Reynolds number requirement is not satisfied in the low-speed test section. However, the test in the High-speed test section at various flow velocities make it possible to check the dependence of the results on the Reynolds number.

The blockage ratio X_b has to be defined at a yaw angle of 30° (X_{b30}). This is calculated as the ratio of the total modelled (train model + scenario) configuration's projected side area to the wind tunnel's cross section. In Table 2 the highest blockage value recorded in the tests, i.e. in presence of the higher windbreaks, is indicated.

In compliance with the requirement of the EN standard, the blockage ratio is always smaller than 15%. According to the standards, for the close section with this value of blockage ratio, no blockage correction is needed because the coefficients are overestimated and therefore it is conservative not to apply a correction here.

On the other hand, in order to verify the effect of the blockage on the aerodynamic coefficients and to compare the coefficients measured in the different test sections, they must be evaluated with blockage correction.
The blockage correction applied is indicated in the EN 14067-4 regulation [5] and leads to a correction of the wind speed (V) used to calculate the aerodynamic coefficients and pressure coefficients (see section 2.4):

$$V_{corr} = \sqrt{1 + X_b} * V \quad (1)$$

Table 2: Constraints for performing wind tunnel tests compliant with the EN standard: limit values and values in the actual wind tunnel tests.

Parameter	Limit value full scale	Limit value 1:15 scale	Measured value in low-speed test section	Measured value in high-speed test section
D	8000 mm	533 mm	4626 mm	627 mm
L_{Train}/L_w	0.75	0.75	0.19	0.65
$\delta_{99\%}$	< 30% of vehicle height	80 mm	80 mm	40 mm
Re	$2.5\ 10^5$	$2.5\ 10^5$	$1.7\ 10^5$	$6.7\ 10^5$
Iu	2.5%	2.5%	2%	0.15%
X_{b30}	15%	15%	3.08%	8.11%

2.2 Train, windbreak, and infrastructure scenario models

The train model tested is the ETR1000. All the dimensions of the original vehicle were reduced to a 1:15 scale ratio, to obtain geometric similarity to the real train. The train model consists of:

- First vehicle, fitted with an internal 6-component dynamometric balance for force and moment measurements and pressure taps.
- Half of the second vehicle, placed downstream of the first vehicle as a boundary condition (in compliance with the requirement of the EN 14067-6 standard).

The space between the two vehicles was reproduced with the correct separation that is found on the real train, and the mechanical contact between the tested model (first vehicle) and the second vehicle is always excluded. The geometry of the wind tunnel model was reproduced as prescribed by the EN 14067-6 standard, approximating the geometry of the bogies and avoiding the pantographs. An overview of the train model is visible in Figure 1. In particular, the gap between the train's underbody and the top of the rail, and the gap between the two vehicles are highlighted. The main dimensions of the scaled first vehicle are (length, width and height): 1723.1 mm, 253.7 mm and 192.4 mm. The half second vehicle length is 856.9 mm.

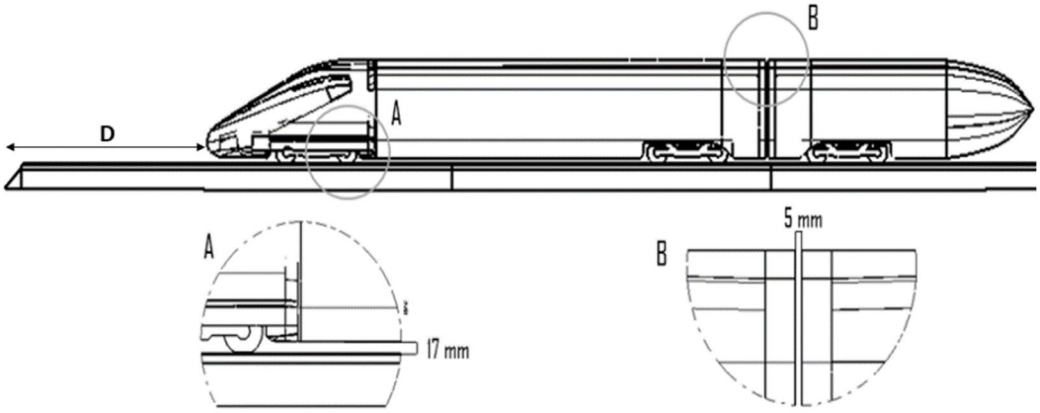

Figure 1: lateral view of the train model.

Several infrastructure scenarios were reproduced: from the standard "Single track ballast and rails" (STBR) and "Double track ballast and rails" (DTBR), to DTBR with the addition of one or two rows of solid (BS: porosity P = 0%) or porous (BP: porosity P = 40%) windbreaks, of different heights: 1, 1.5 and 2 m from top of the rail (TOR). The distance of the windbreaks in relation to the train's symmetry plane is equal to 4.2 m (full-scale). Figure 2 shows the main dimensions of BS, BP (at a single height), their arrangement in longitudinal modules 6 m in length and an example of configuration with DTBR and two rows (upwind and downwind) of 2 m BP.

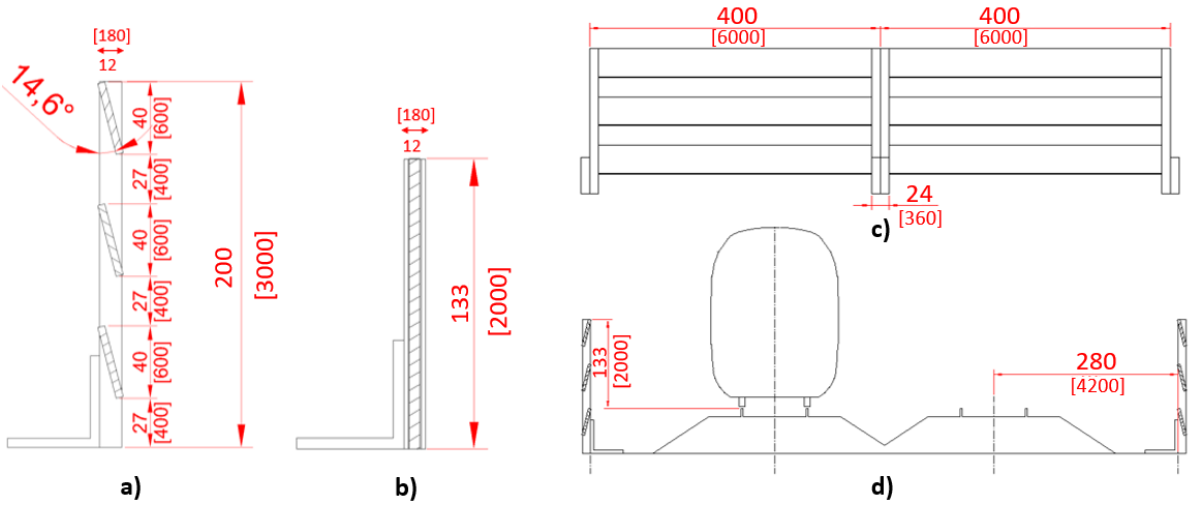

Figure 2: a) porous windbreaks (BP); b) solid windbreaks (BS); c) longitudinal windbreak module; d) example of test configuration. Model and full-scale (in-brackets) distances (dimensions in mm).

Figure 3 and Figure 4 show a top view of the experimental setup with the same scenario (DTBR with barriers) in the high-speed and low-speed test sections respectively. Due to the larger size of the low-speed test section, the length of the row of barriers in front of the train is longer (4626 mm) than in the high-speed section setup (627 mm). The direction from which the wind is coming for positive yaw angles (I.e. the upwind side) can identified by the track on which the train is placed. As indicated also in Figure 6, the inclined wind always come from the region where there is no track and the first track that the wind encounters is the one above which the train is placed.

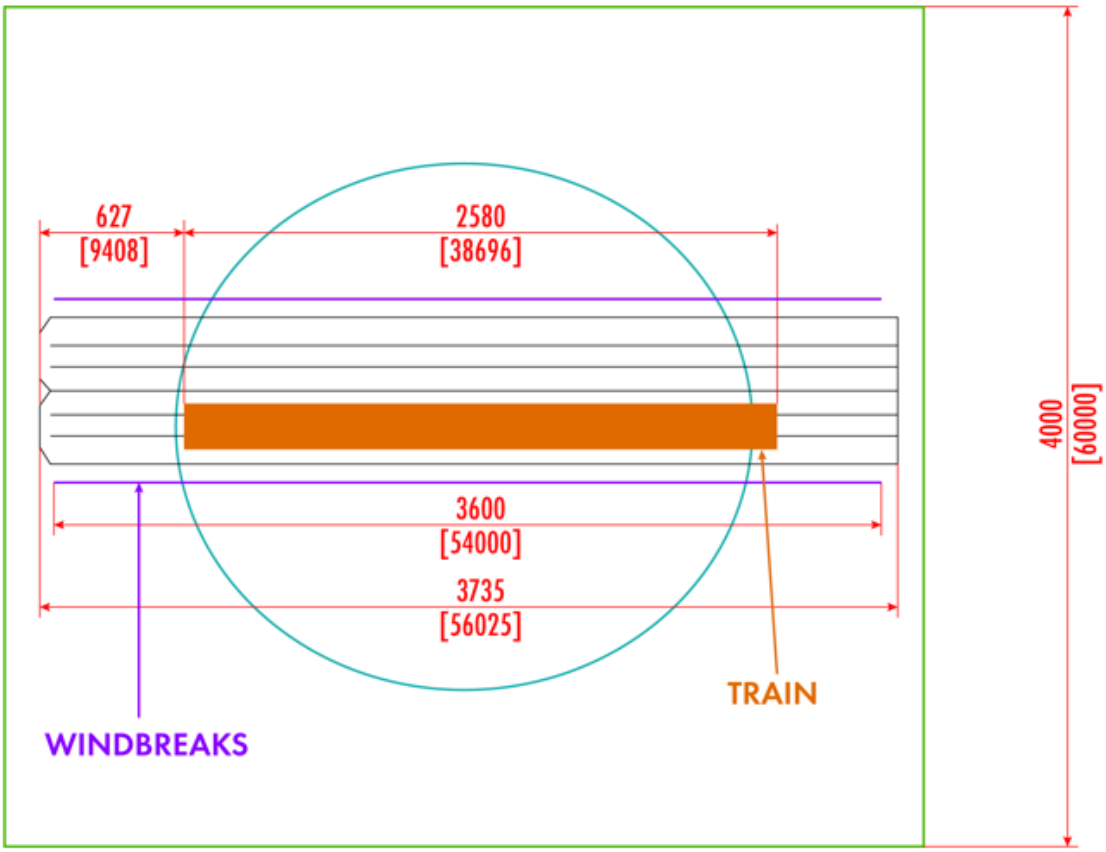

Figure 3 - High-speed test section, DTBR scenario with windbreaks, top view: model and full-scale (in-brackets) distances (dimensions in mm).

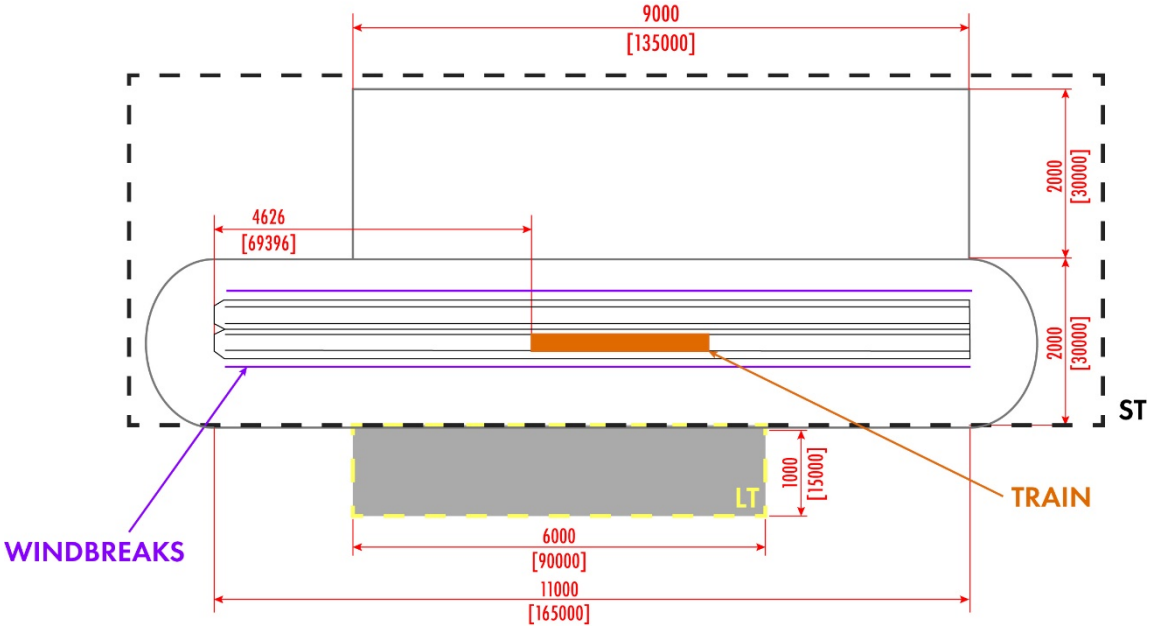

Figure 4: - Low-speed test section, DTBR scenario with windbreaks, top view: model and full-scale (in-brackets) distances (dimensions in mm).

As shown in Figure 4, in the low-speed test section, it is possible to perform measurements with only the standard splitter plate (ST) or by adding (upwind side) an appendix (LT) to it. In this way it is possible to study the effect of different widths of splitter plate for high yaw angles of the flow. An overview of

the experimental setup of high-speed test section and low-speed test section respectively is shown in Figure 5.

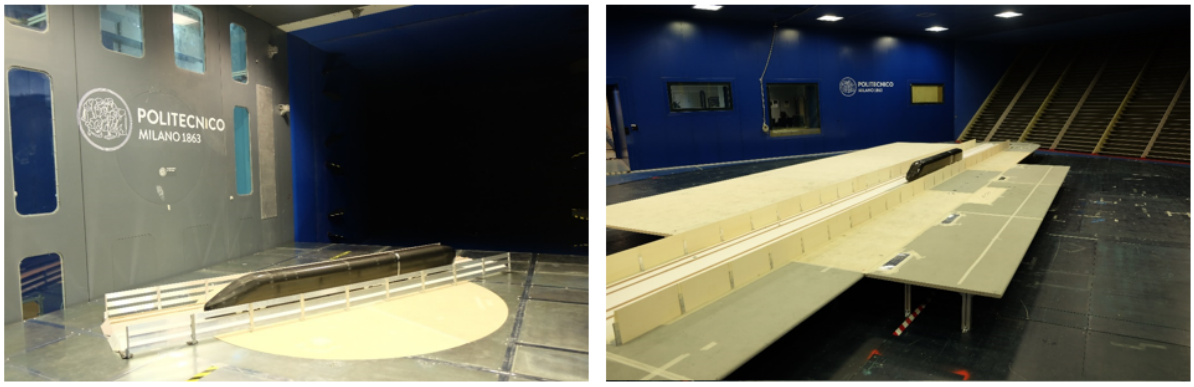

a) b)

Figure 5: Experimental setup in high-speed test section (a) and low-speed test section (b).

2.3 Test configurations

The final aim of this study is to evaluate the effects of different wind tunnel configurations on the measurement of the aerodynamic coefficients of a train in the presence of windbreaks. In particular, the following parameters were considered:

- Wind speed/Reynolds number: the tests in the high-speed test section were carried out at three different wind speeds (V = 13, 30, 50 m/s), while in the low-speed test section the tests were performed at 13 m/s.
- Length of the windbreaks in front of the train: 627 mm in the high-speed test section and 4626 mm in the low-speed test section (from the train's nose).
- Width of the splitter plate: 2 m in the high-speed test section; 1 m (ST) and 2 m (ST + LT) in the low-speed test section (from the train's longitudinal axis).
- Turbulence intensity: in the low-speed test section, two different atmospheric boundary layers were simulated: smooth flow conditions (without turbulence generators, Iu=2%) and a mean turbulence condition, characterised by a turbulence intensity of 10%. In the high-speed test section, the turbulence intensity is equal to Iu=0.15%. As a consequence, a total of three turbulence conditions were tested.
- Array of windbreak barriers: in the low-speed test section, only one windbreak (upwind side) array and two (upwind + downwind side) arrays were tested.

The parameters listed above were tested in the presence of solid windbreaks (BS), porous windbreaks (BP) and without windbreaks. Table 3 summarizes all the tests carried out.

285 *Table 3: summary of all wind tunnel tests carried out.*

	Test number	Scenario	Windbreak type	Windbreak height (m)	Splitter plate	Windbreak rows	Wind speed (m/s)	Turbulence Intensity (%)
High-speed	1	STBR	NO	-	-	-	13	0.15
	2	STBR	NO				30	0.15
	3	STBR	NO				50	0.15
	4	DTBR	NO	-	-	-	13	0.15
	5	DTBR	NO	-	-	-	30	0.15
	6	DTBR	NO	-	-	-	50	0.15
	7	DTBR	Solid (P=0%)	1.5	-	Upwind and downwind	13	0.15
	8	DTBR	Solid (P=0%)	1.5	-	Upwind and downwind	30	0.15
	9	DTBR	Solid (P=0%)	1.5	-	Upwind and downwind	50	0.15
	10	DTBR	Porous(P=40%)	2	-	Upwind and downwind	13	0.15
	11	DTBR	Porous(P=40%)	2	-	Upwind and downwind	30	0.15
	12	DTBR	Porous(P=40%)	2	-	Upwind and downwind	50	0.15
Low-speed	13	DTBR	NO	-	-	-	13	2
	14	DTBR	NO	-	-	-	13	10
	15	DTBR	Solid (P=0%)	1	ST	Upwind and downwind	13	2
	16	DTBR	Solid (P=0%)	1	ST + LT	Upwind and downwind	13	2
	17	DTBR	Solid (P=0%)	1.5	ST	Upwind and downwind, only upwind	13	2
	18	DTBR	Solid (P=0%)	1.5	ST + LT	Upwind and downwind	13	2
	19	DTBR	Solid (P=0%)	1.5	ST + LT	Only upwind	13	2
	20	DTBR	Solid (P=0%)	2	ST	Upwind and downwind	13	2
	21	DTBR	Solid (P=0%)	2	ST+LT	Upwind and downwind	13	2
	22	DTBR	Solid (P=0%)	2	ST+LT	Upwind and downwind	13	10
	23	DTBR	Porous (P=40%)	2	ST	Upwind and downwind	13	2
	24	DTBR	Porous (P=40%)	2	ST + LT	Upwind and downwind	13	2
	25	DTBR	Porous (P=40%)	2	ST + LT	Upwind and downwind	13	10

286

287

2.4 Measurement setup and conventions

During all the tests carried out in the two test sections, force/moments and pressure were measured. In particular, for measuring the forces and moments a dynamometric balance was placed inside the train model. Force aerodynamic coefficients are defined according to EN 14067-6:

$$C_{F_i} = \frac{F_i}{1/2\,\rho A {V_{corr}}^2} \qquad i = x, y, z \tag{2}$$

$$C_{M_i} = \frac{M_i}{1/2\,\rho A h {V_{corr}}^2} \qquad i = x, y, z \tag{3}$$

$$C_{M_{x,lee}} = \frac{M_x - F_z s}{1/2\,\rho A h {V_{corr}}^2} = C_{M_x} - C_{F_z}\frac{s}{h} \tag{4}$$

where Fi (i = x, y, z) are the components of the aerodynamic force in the reference system and Mi (i = x, y, z) are the corresponding moments. ρ is the air density, V is the corrected wind speed that takes the blockage effect into account (see section 2.1), h is equal to 3m (full-scale) and A is a standard reference surface area equal to 10 m^2 (full-scale). The reference system adopted for defining the aerodynamic coefficients (according to EN 14067-6) was fixed to the vehicle and its origin coincided with the centre of the vehicle at the level of the top of the rail: the longitudinal axis *x* is oriented in the direction of travel, the *z* axis is vertical and directly downwards, and the *y*-axis is perpendicularly oriented to form a right-handed coordinate system. The reference system is shown in Figure 6, where the yaw angle β_w of the train in relation to the wind direction is also represented. Figure 6 reports also the point for the CMxlee calculation.

160 pressure taps were formed on the train, in order to detect the static pressure. Pressure taps are arranged in rings along the train and their positions are indicated in Figure 7. Pressure taps distribution in the sections is visible in the pressure plot in the following (Figure 10,12,14 etc): every point from which an arrow starts corresponds to a pressure tap.

Depending on the position, the rings contain a variable number of measuring points, of up to 21, as can be seen in the figures in section 3.

The pressure coefficients are defined according to EN14067-6:

$$C_p = \frac{\overline{P - P_\infty}}{1/2\rho {V_{corr}}^2} \tag{5}$$

where $\overline{P - P_\infty}$ is the mean value of the differential pressure measured by the pressure tap considered. The static pressure measured in the test section was taken, as a reference pressure P_∞.

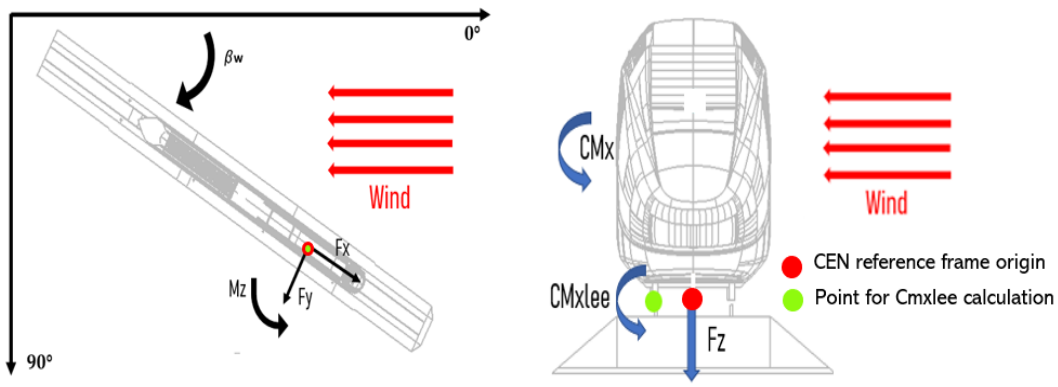

Figure 6 - Reference frame for the aerodynamic force/moment coefficients and angle of attack.

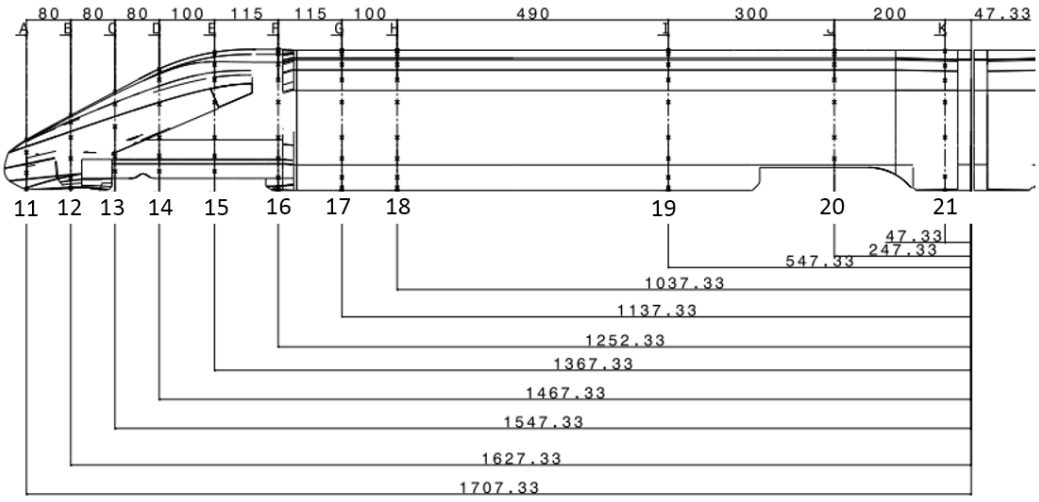

Figure 7: Pressure tap positions along the train. Dimensions in mm.

3 Results

In this section the main aerodynamic coefficients (CFy, CFz, CMx, CMxlee) related to the safety of high-speed trains will be shown. The attention focuses on the effects of the different parameters on the aerodynamic coefficients measured.

In particular, in sub-section 3.1, 3.2, 3.3, the effects of the parameters related to the flow characteristics are be evaluated:

- Reynolds number.
- Turbulence intensity.
- Boundary layer profile.

In sub-section 3.4, 3.5, 3.6 the effects of the parameters related the geometric characteristics of the experimental setup are evaluated:

- Width of the splitter plate on which the infrastructure scenario is set.
- Length of the windbreaks in front of the train.
- Presence of windbreak barriers on both sides of the train or only the upwind side.

Finally, guidelines for carrying out wind tunnel tests on railway vehicles in the presence of windbreak barriers are proposed, in order to prevent scaled setup errors and reproduce the full-scale train conditions as closely as possible.

3.1 Reynolds number

In this paragraph, the effect of Re number is shown for the following configurations:

- STBR, without windbreaks, in the HS test section (test numbers 1, 2, 3 see Table 3).
- DTBR, without windbreaks, in the HS and LS test sections (test numbers 4,5,6,12).
- Solid windbreaks (BS) 1.5 m high in the HS test section (test numbers 7,8,9).
- Porous windbreaks (BP) 2 m high, and 1.5 m solid windbreaks (BS), in the HS test section. (test numbers 10,11,12).

Figure 8 shows the effect of the Re number on the coefficients measured in the high-speed test section, with an STBR scenario, without windbreaks, while Figure 9 shows the same effect on the aerodynamic coefficients measured in both the low-speed and high-speed test sections with the DTBR scenario without windbreak barriers.

Contrary to what was found for other train geometries in the same wind tunnel [7] or in other wind tunnels [21], for the ETR1000 train considered, with both the scenarios, it is possible to identify, two sets of curves by varying the Re number, that differ in the range β_w = 60°-80° while showing very similar values for low yaw angles and when the flow becomes perpendicular to the model.

In the high-speed test section, with both the scenarios, the set that reaches a CMxlee peak value at 60°-65° includes the two curves at the lower Re numbers, while the set that shows a maximum value at 45°-50°, characterised by a smoother trend, includes the curve at Re=6.7 10^5 (V=50 m/s). This coefficients behaviour for different Reynolds numbers, will be defined in the following as “double behaviour”.

In the low-speed test section, the coefficients measured at the lower Re number show a behaviour similar to that found in the high-speed test section at the two lower Re numbers, but only up to a yaw angle β_w =70°. Over this angle, the trend decreases with a lower slope or remains constant, leading, at β_w =90°, to significantly higher C_{Fy} and C_{Mx} coefficients and to a significantly lower C_{Fz} coefficient. These two opposite contributions compensate and, on the contrary, the CMxlee was found to be very similar to those measured for the same angle in the other wind tunnel section.

It is supposed that the cause of this behaviour is due to phenomena related to aerodynamic hysteresis [22]. For flows with thick boundary layers and transitional separation bubbles, non-linearities in the force coefficient curves that depend on the flow history may appear. In these tests the data for the low-speed test section were acquired with a different history due to the wind tunnel procedure (i.e. cooling of the test section, ramp up to the regime wind speed), compared to the data acquired in the high-speed test section. This fact, according to the authors opinion, could have determined some difference in the high yaw angle coefficients.

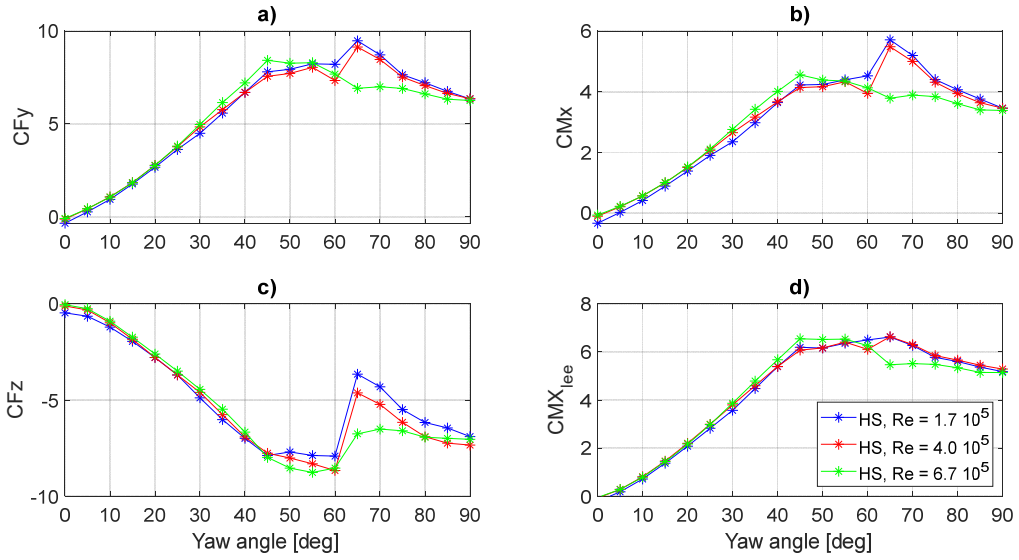

401

Figure 8: STBR, no windbreaks, high-speed (HS) test section, lateral force (a), rolling moment (b), vertical force (c) and lee-rail rolling moment (d) aerodynamic coefficients for different Re numbers as a function of the yaw angle b_w.

402

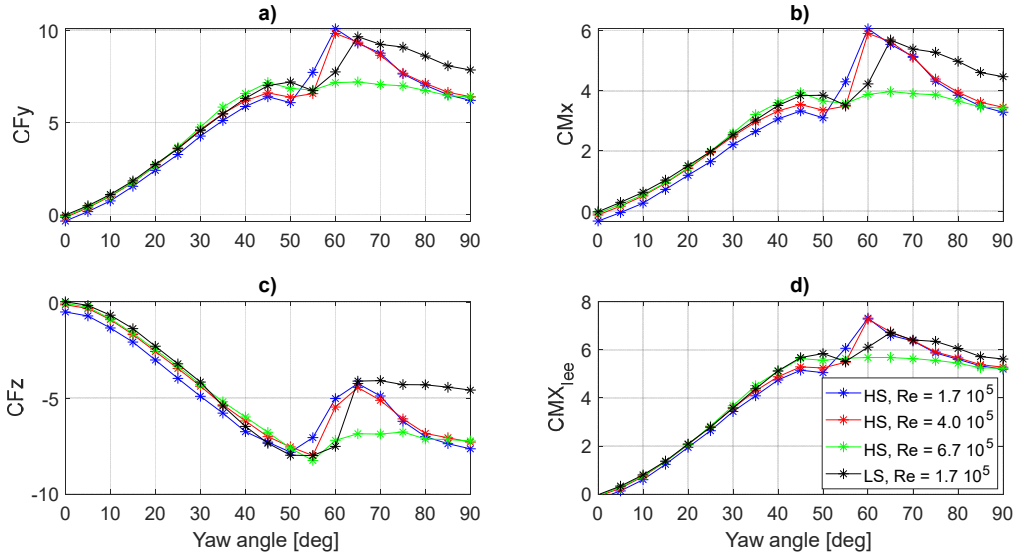

Figure 9: DTBR, no windbreaks, low-speed test section (LS) and high-Speed (HS) test section, lateral force (a), rolling moment (b), vertical force (c) and lee-rail rolling moment (d) aerodynamic coefficients for different Re numbers as a function of the yaw angle β_w.

403

404 As regards the effects observed in the high-speed test section, each set of curves is characterized by a
405 different flow organization and occurs depending on the Re number. In particular, as shown by the
406 pressure distributions plotted in Figure 10 for β_w =70° and the DTBR scenario, the double behaviour of
407 the force/moment aerodynamic coefficients is due to a different distribution of the flow in the middle
408 region of the train's body (after the nose and before the vehicle's end, sections 17, 18, 19). In this
409 region, only the coefficients measured with the highest Re number show an underpressure peak at the
410 upwind corner, that is responsible for the lower lateral force and rolling moment coefficient and the
411 higher vertical force coefficient. Outside of this region (sections 15 20 21), the flow field measured
412 with the three velocities returns to being similar. Similar results were also found for the STBR scenario.

The reason for the double behaviour observed is associated with the combination of the Reynolds number, which characterizes the fluid-dynamic phenomenology of the object, and the particular geometry of the train, with smooth rounded edges and smooth surfaces.
From the safety point of view, the double behaviour appears in a range of yaw angles which are not determinant for the definition of the CWCs of a high-speed train to crosswind action (typical significant angles for high-speed trains are 0°-30°). However, if conventional trains (V_{max} lower than 200 km/h) are involved, coefficients in the range between 60° and 80° can have an impact on the CWCs and thus correct simulation of the full-scale train's aerodynamic behaviour at these high yaw angles as well, becomes mandatory. For these cases, tests at high Re numbers should therefore be recommended.

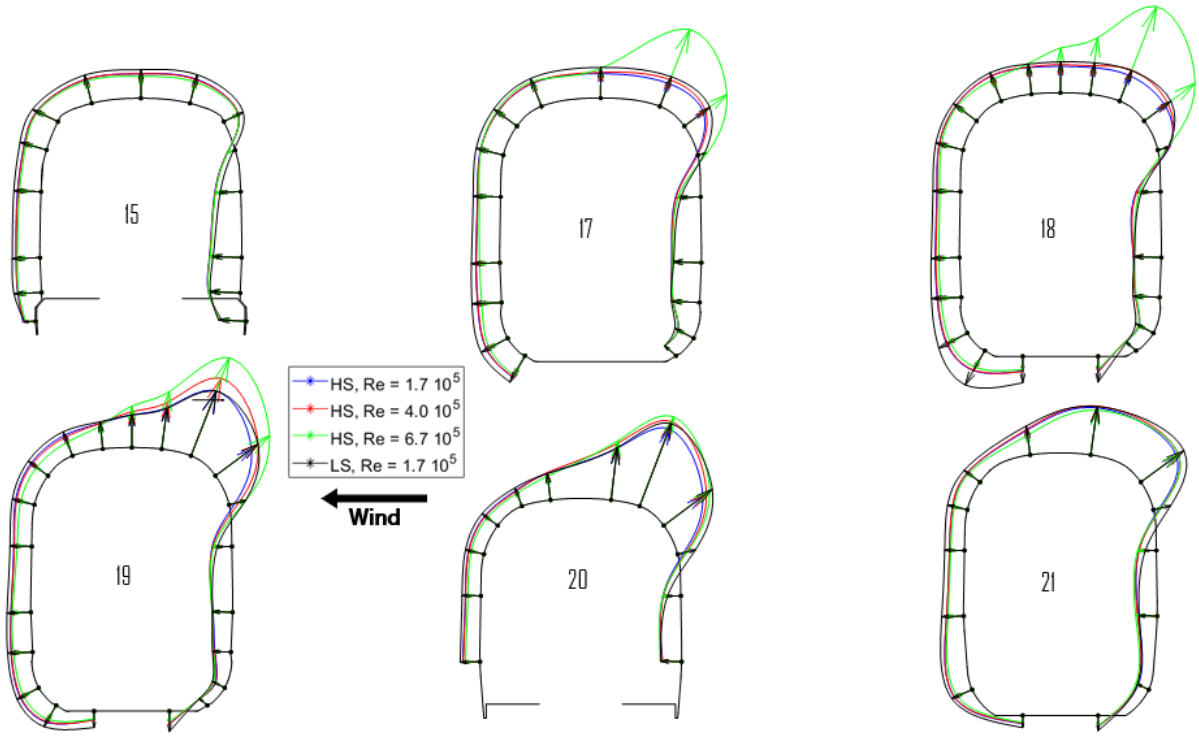

Figure 10: DTBR, no windbreak, low-speed test section (LS) and high-speed (HS) test section, pressure coefficients for different Re numbers and β_w = 70°.

As far as the coefficients measured in the low-speed test section are concerned, Figure 9 shows that these coefficients (black line), measured at 13 m/s, in the range 0°-60°, are equivalent to those found in the high-speed test section at the highest Re number (green line) while there is a gap in relation to the corresponding coefficients measured in the high-speed test section at the same velocity (blue line). This result can be justified by considering that, as will be investigated in greater depth below (see Figure 12), the higher turbulence in the low-speed test section contributes to increasing the local Re number [23].
Finally, Figure 11 shows the force and moment coefficients measured with solid and porous windbreaks for different wind speeds in the high-speed test section: it is possible to see that the Reynolds number's effect at low yaw angles occurs even in the presence of windbreaks, but to a much lesser extent as the double behaviour at around 50°-60° with barriers does not show up. In fact, the windbreaks, by filtering the incident flow and introducing a higher local turbulence intensity, prevent the occurrence of the different behaviours of the flow seen previously as a function of the Re number. Thus, in the presence of windbreaks, even for trains characterised by smooth edges and surfaces, the double behaviour of the flow observed without barriers, that leads to a significant difference in the

coefficients around the maximum values, does not occur and, even for low Reynolds numbers, the errors compared to the true full-scale coefficients will be limited.
In conclusion, the windbreaks addition decreases the Reynolds dependency of the train aerodynamic coefficients.

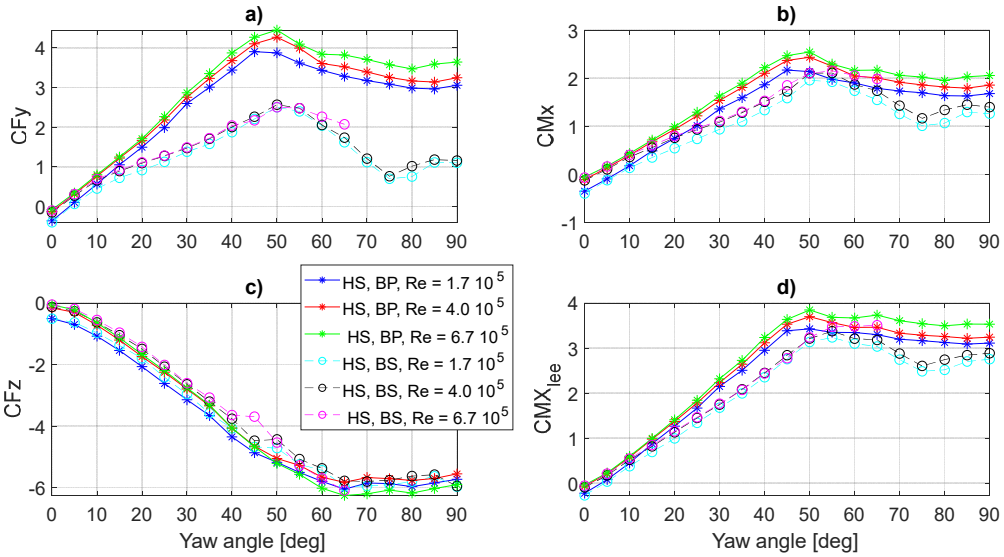

Figure 11: Solid windbreaks (BS) and porous windbreaks (BP), low-speed test section (LS) and high-speed (HS) test section, lateral force (a), rolling moment (b), vertical force (c) and lee-rail rolling moment (d) aerodynamic coefficients for different Re numbers as a function of the yaw angle β_w.

3.2 Turbulence intensity

The effect of the turbulence is shown in this paragraph by comparing the following configurations:

- DTBR, without windbreaks, low (Iu=0.15%) turbulence conditions, HS test section (test number 6 see Table 3).
- DTBR, without windbreaks, low (Iu=2%) and high (Iu=10%) turbulence conditions, LS test section (test numbers 13, 14).
- Solid windbreaks (BS) 2 m high, low (Iu=2%) and high (Iu=10%) turbulence conditions, LS test section (test numbers 21, 22).
- Porous windbreaks (BP) 2 m high, low (Iu=2%) and high (Iu=10%) turbulence conditions, LS test section (test numbers 24, 25).

Figure 12 shows the coefficients measured with different levels of turbulence in the three configurations characterised by no windbreaks, porous and solid windbreaks: it is possible to see that the addition of turbulence in the incoming flow from 2% to 10% in the low-speed test section does not lead to significant differences for the tests with windbreaks.
As explained in paragraph 3.1, at high yaw angles, for the configurations without barriers (STBR and DTBR), the Reynolds number effect induces a double behaviour that leads to significant differences between the coefficients, like those observed in Figure 9 between the blue and green lines for $b_w > 50°$. Figure 12 shows that without windbreaks, the addition of turbulence results in an increase in the local Re number and makes it possible to obtain the same coefficients as those measured in the HS test section with the highest Reynolds number, as also shown by the pressure coefficient distributions laid out in Figure 13.

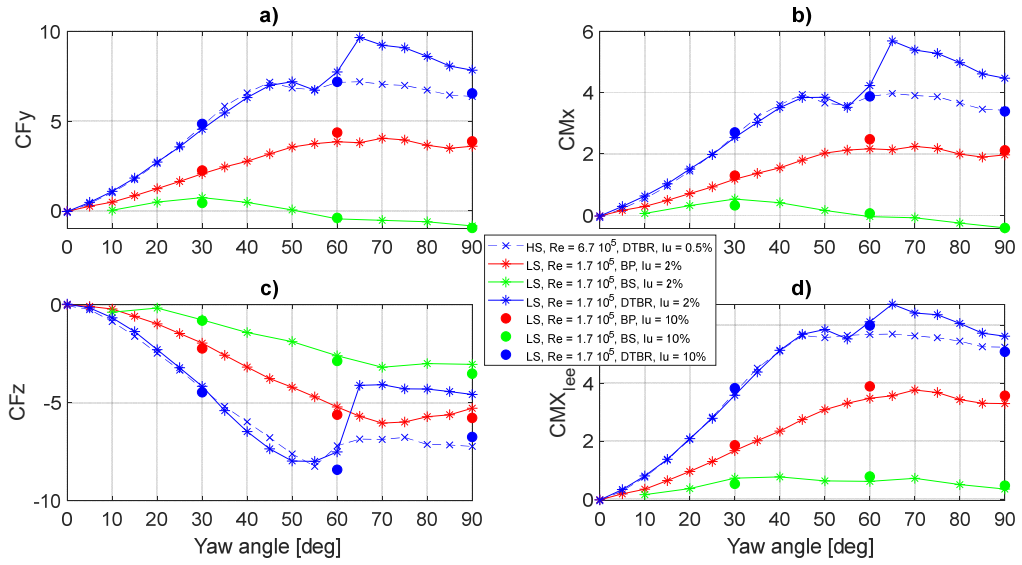

Figure 12: DTBR, no windbreaks, solid windbreaks (BS) and porous windbreaks (BP), low-speed test section (LS) and high-speed (HS) test section, lateral force (a), rolling moment (b), vertical force (c) and lee-rail rolling moment (d) aerodynamic coefficients for different turbulence intensity Iu as a function of the yaw angle β_w.

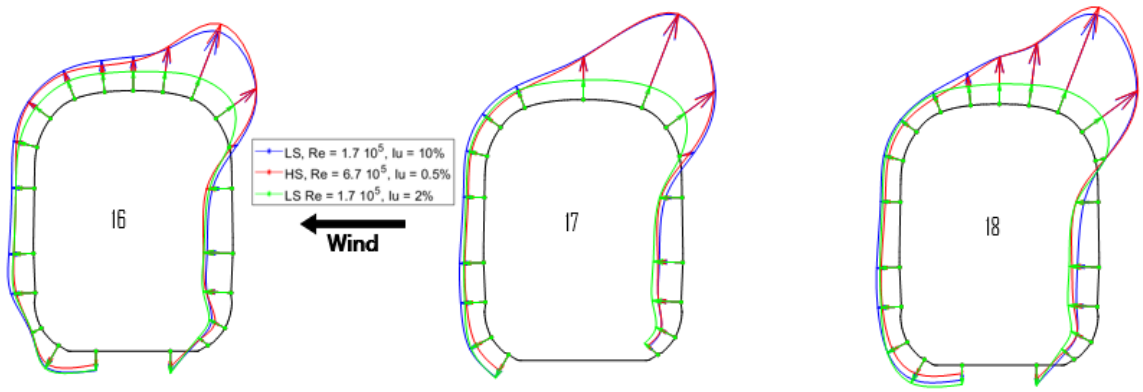

Figure 13: DTBR, no windbreak, low-speed test section (LS) and high-speed (HS) test section, pressure coefficients for different Re numbers and β_w = 90°.

3.3 *Boundary layer profile*

As explained in section 2, the train model was subjected to a different boundary profile in the two test sections. The effect of the difference in the velocity profile can be seen in the train sections that are not affected by the double aerodynamic behaviour associated with the Re number.
The effect of the turbulence is shown in this paragraph by comparing the following configurations:

- DTBR, without windbreaks, in HS and LS test section (test numbers 4, 14 see Table 3).
- Solid windbreaks (BS) 1.5 m high, in HS and LS test section (test numbers 7, 18).
- Porous windbreaks (BP) 2 m high, in HS and LS test section (test numbers 10, 24).

Figure 14 show the pressure coefficient for the same train section 21 for DTBR, porous barrier (BP), and solid barrier (BS) configurations.
Without barriers in the low-speed test section there is a lower upwind push (right part of the train section), due to the greater height of the boundary layer on the supporting table (80 mm height vs 40 mm height in the high-speed test section), with a consequent lower positive pressure coefficient.
This effect is reduced with porous barriers (BP), while the boundary layer profile has no influence on the results in the case of solid barriers (BS), where, in the area between the barrier and the train, a negative pressure is generated by the wake of the barrier: the pressures in this area therefore depend on the wake of the barrier and don't depend on the incident boundary layer profile.

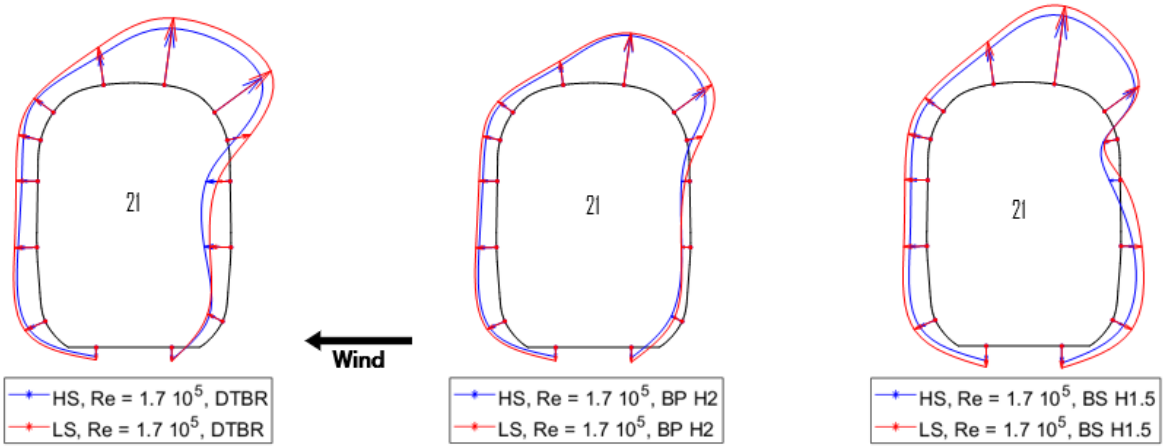

Figure 14: DTBR, no windbreak, low-speed test section (LS) and high-speed (HS) test section, pressure coefficients in the presence of different boundary layer and $\beta_w = 90°$.

3.4 Width of the splitter plate

In this section, the effect of the width of the splitter plate upwind of the vehicle model will be analysed by considering the following configurations:

- Solid windbreaks, in LS test section, standard width of the splitter plate (ST) (test numbers 15 16, 17, 18, 20, 21 see Table 3).
- Porous windbreaks, in LS test section, splitter plate plus appendix (ST + LT) (test numbers 23 24).

In all these configurations, the length of the windbreak barriers are the same.
Figure 12 shows the results collected in the low-speed test section with solid barriers (BS) of different heights: for each barrier height, coefficients have been measured with the standard splitter plate (ST) and with the additional plate (ST + LT).
For all windbreak heights tested, marked differences in the coefficients measured for high yaw angles are visible. On the contrary, no discrepancy was found up to $\beta_w = 30°$.
These results can be explained by the fact that, at low yaw angles, the most important part of the surrounding scenario, from which the flow that then goes towards the train passes, is the scenario in front of the train, that is equal both in the case of ST and ST+LT; on the contrary, for high yaw angles, the flow that reaches the train comes from the lateral part of the surrounding.
For all windbreak heights, a reduced width of the splitter plate (ST) causes marked differences in the incident wind profile, due to the vortical structures that form between the edge of the table and the beginning of the windbreaks. The solid barriers do not allow air to pass through, creating a region of

overpressure in front of the barriers. As the lateral supporting table has a short length, the overpressure modifies the flow angle and intensity of the upstream wind's speed profile when it reaches the table.

For this reason, a flow separation occurs at the edge of the splitter plate. A single large vortex, induced by the separation of the flow, forms between the edge of the table and the edge of the upwind windbreak.

This big vortex produces a significative wind speed in the vertical direction, that increases the wake behind the barriers and, consequently, decreases the forces and moments on train.

The magnitude of the differences in the coefficients for SL and ST+LT configurations depends on the height of the windbreaks, because the wake shape behind the windbreaks changes with the barrier height.

In conclusion, wind tunnel tests with solid barriers can lead to the evaluation of forces and moments that are significantly different from real full-scale ones, especially when the splitter plate in the upwind direction is not sufficiently wide. In particular, in this case, it was demonstrated that an upwind width of the splitter plate equal to about 3.75*H (being H the vehicle height) is not sufficient to obtain results that are representative of the real conditions. This conclusion is linked to the specific geometry of the windbreaks (in particular their height) but focuses on an aspect of the experimental setup that must be verified in order to achieve reliable measurements.

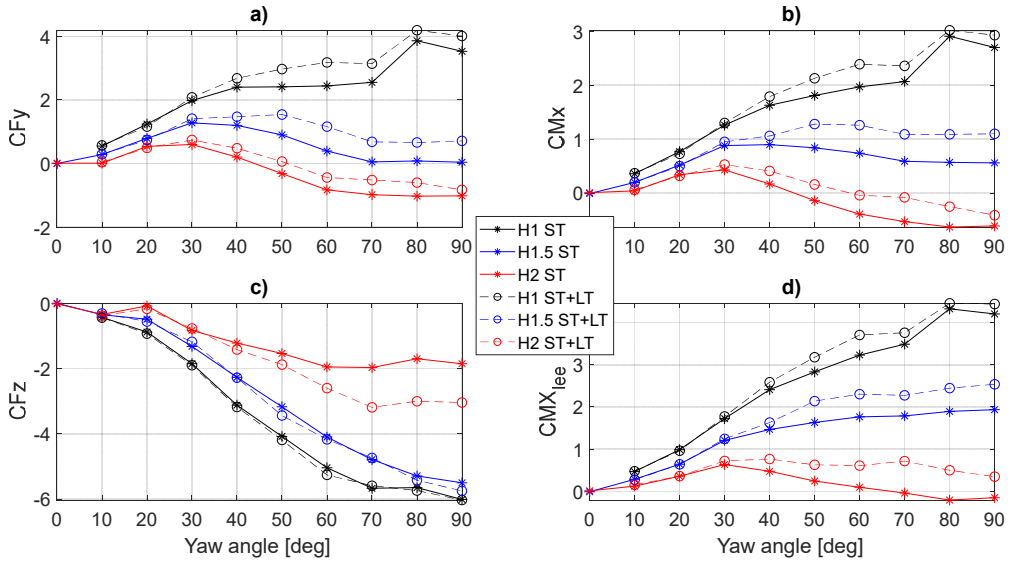

Figure 12: solid windbreaks (BS) of different heights, low-speed test section (LS), lateral force (a), rolling moment (b), vertical force (c) and lee-rail rolling moment (d) aerodynamic coefficients for different splitter plates as a function of the yaw angle β_w.

Figure 13 shows the results collected for porous barriers (BP) 2m high, tested in the low-speed test section with the standard splitter plate (ST) and the splitter plate plus the appendix (ST+LT). In this case, there are no differences in the measured coefficients. The porous barriers allow air to pass through: as a consequence, the flow separation at the edge of the table does not occur (event at high yaw angles), because the overpressure in front of the barriers is significant lower.

In conclusion, for tests with porous barriers, a splitter plate 3.75*H wide is sufficient to correctly represent the real conditions.

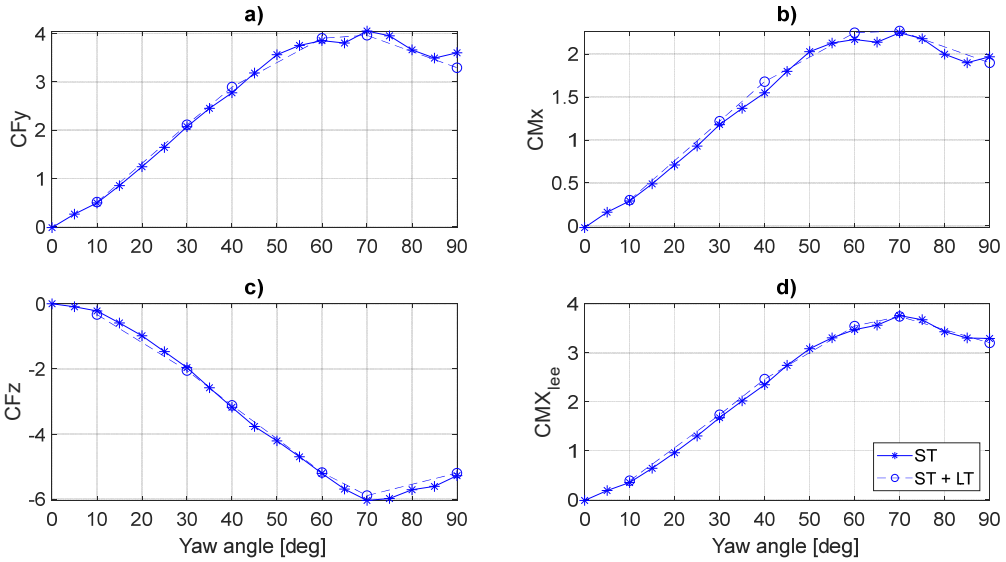

Figure 13: porous windbreaks (BP), low-speed test section (LS), lateral force (a), rolling moment (b), vertical force (c) and lee-rail rolling moment (d) aerodynamic coefficients for different splitter plates as a function of the yaw angle β_w.

547
548

549 ### *3.5 Length of the windbreaks in front of the train*

550 The effect of the length of windbreak barriers in front of the train model will be studied by comparing
551 the following configurations:
552
553 - Solid barriers (BS) 1.5 m high, in HS and LS test section (test numbers 7, 18 see Table 3).
554 - Porous barriers (BP) 2 m high, in HS and LS test section (test numbers 10, 24).
555
556 It is possible to observe the influence of the length of the windbreaks in front of the train by comparing
557 the high-speed and low-speed test section results. In fact, the length of the windbreaks, measured
558 from the nose of the train, in the low-speed test section (L_b=627mm) is about 2.35*H , more than 7
559 times shorter than that of the barriers in the high-speed test section that is about 17.35*H
560 (L_b=4626mm), as shown in Figure 3 and Figure 4.
561 Figure 14 shows the force/moment aerodynamic coefficients measured with porous barriers (BP) for
562 V=13 m/s in the high-speed and low-speed test sections.
563
564
565
566
567
568
569
570
571
572
573

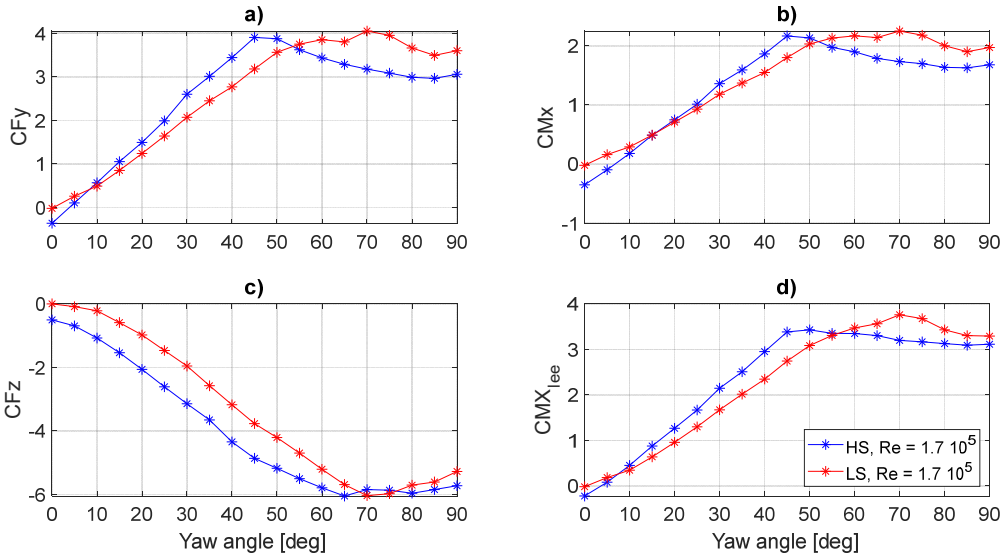

Figure 14: porous windbreaks (BP), low-speed (LS) and high-speed (HS) test section, lateral force (a), rolling moment (b), vertical force (c) and lee-rail rolling moment (d) aerodynamic coefficients as a function of the yaw angle β_w.

It is possible to see that, for high angles of attack (greater than $\beta_w = 60°$), the coefficients measured in the LS test section are higher respect to those measured in the HS test section.
The reason is the Reynolds number effect discussed in Figure 11. The coefficients measured in the LS test section (at V=13 m/s) are equivalent to those measured in the HS test section at the highest velocity (V=50 m/s) and this effect can be justified by considering the higher turbulence of the LS section that leads to a corresponding greater local Re number, as seen for the configuration without a barrier in the previous section.
Anyway, for angles between $\beta_w = 10°$ and $\beta_w = 60°$, due to the shorter length of barriers in the HS test section and the consequent lower shielding effect, the flow produces a higher pressure on the train model and causes an increase in the coefficients. This effect is also visible from the pressure coefficients shown in Figure 15.
On the windward side of the train (right part of the section) it is possible to see, for all the sections, a higher positive pressure for the tests carried out in the high-speed test section; this pressure is responsible for the greater lateral force and rolling moment coefficients measured with this configuration.
Furthermore, one can see that this pushing effect decreases in the direction of the train's tail, i.e. moving from section 12 to section 21. On the first rings of the train starting from the nose, there is a greater effect of thrust on the windward side, while this effect decreases as it approaches the train's tail, confirming that the cause of this effect is due to the length of the barriers in front of the train.
The high differences in CFz coefficients mainly depend on the reduction of the depression peak on the leeward side in the train nose region.
Furthermore, in the high-speed test section at very low yaw angles, up to $\beta_w = 10°$, there is an unrealistic channelling of the flow that increases all the aerodynamic coefficients measured and creates asymmetry in the flow at $\beta_w = 0°$, resulting in a CFy different from zero.

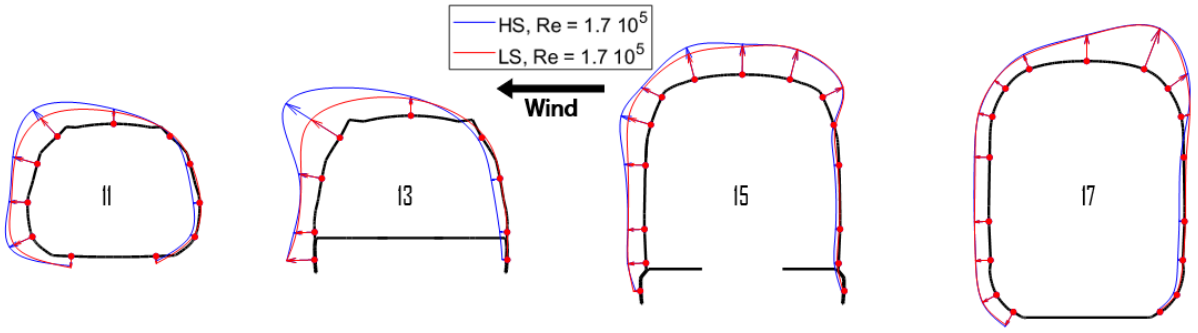

Figure 15: porous windbreaks (BP), low-speed test section (LS) and high-speed (HS) test section, pressure coefficients in presence of different windbreak lengths and β_w = 40°

similar conclusions can also be drawn by observing the results obtained with solid barriers.
Figure 16 shows the force/moment coefficients measured with solid barriers 1.5m high (BS) for V = 13 m/s in the low-speed and high-speed test sections.
The effects of channelling and different flow shielding due to the different lengths of the barriers in front of the model reproduced in the two test sections is even more evident, as solid barriers do not allow air to pass: differences in the coefficients measured in the two test sections are higher than those observed in the case of porous barriers.
In conclusion, a length of barriers in front of the model equal to 7.35*H is not sufficient to correctly represent real full-scale conditions for porous barriers or solid barriers, especially for the estimation of the coefficients at low yaw angles, and can lead to erroneous conclusions concerning the crosswind safety of high-speed trains as well.

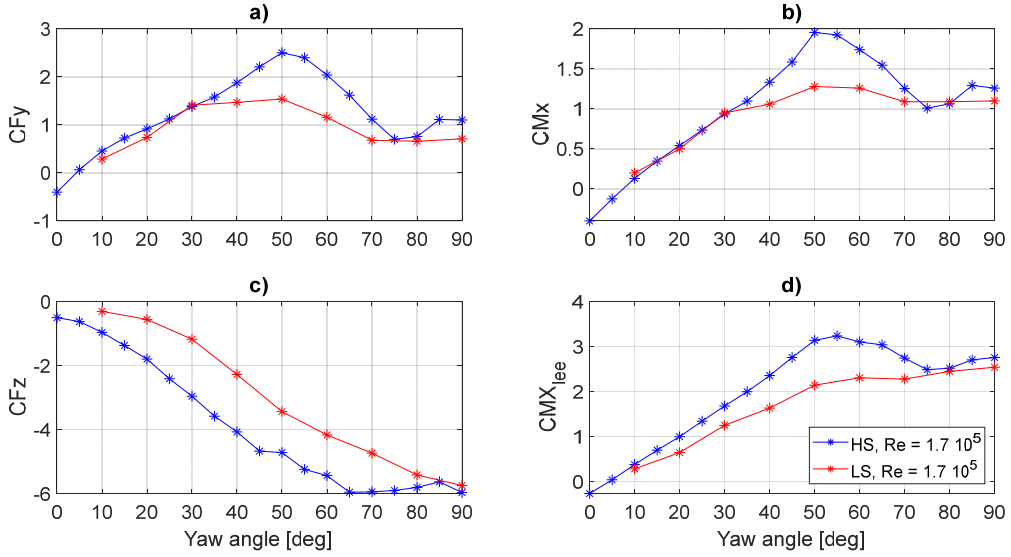

Figure 16: solid windbreaks (BS), low-speed (LS) and high-speed (HS) test section, lateral force (a), rolling moment (b), vertical force (c) and lee-rail rolling moment (d) aerodynamic coefficients as a function of the yaw angle β_w.

3.6 Upwind and downwind rows of windbreaks

The effect of the presence of upwind and downwind rows of windbreaks will be studied by comparing the following configurations:

- Solid barriers (BS) 1.5 m high, in the high-speed (HS) and low-speed (LS) test sections (at different wind velocities) (test number 18,19 see Table 3).

In order to make the experimental setup easier, to check the effects of a windbreak using wind tunnel tests, it would be possible to choose a configuration that reproduces only the upwind row of the barrier, without modelling the downwind one. Or, differently, one could be interested in understanding the extent of the difference, for a site at which the wind direction is constant, between putting only one row of barriers upwind instead of the standard configuration with two rows of fences, upwind and downwind. Below it will be shown how the two configurations lead to differences in the forces acting on the train model.

In particular, in this section the solid barriers, 1.5 m high, tested in the low-speed test section will be considered. An upwind test setup is the configuration with only the upwind row of barriers, while upwind + downwind is a standard setup for the condition with upwind and downwind windbreak barriers.

Figure 17 shows a comparison between these two configurations in terms of force and moment coefficients: it is possible to see that the lateral force and rolling moment coefficients measured with the upwind test setup are lower, for yaw angles higher than 30°, than those measured with the standard setup, while the vertical force coefficients do not show significant differences between the two configurations tested. With the upwind test setup, there is a lower depression in the area of the train's wake, which leads to lower coefficients. This effect can be verified by observing the pressure coefficient distribution in Figure 18 (β_w =60°): the upwind test setup presents, in all the plotted sections, lower negative pressure coefficients in the downwind part of the train (left part) while, on the windward side, the positive pressure coefficients are equivalent for the two configurations considered. On the contrary, on the roof and on the underbody zone, the lower underpressure measured with the upwind test setup compensates, and the total vertical force remains unchanged. The differences in the pressure coefficients are shown at all yaw angles higher than 30°, as the presence of the downwind row of barriers leads to a different structure of the vortex that detaches along the downwind side of the train.

In conclusion, if the real condition is characterised by the standard configuration with barriers upwind and downwind, to get as close as possible to the full-scale situation, we recommend reproducing both rows of windbreaks, to avoid underestimating the effects of fences.

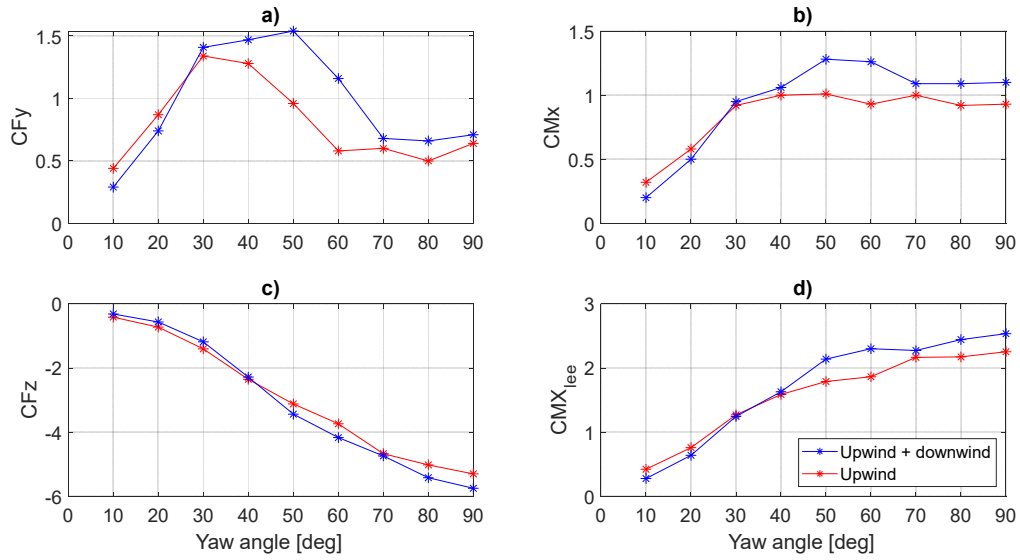

654

Figure 17: solid windbreaks (BS), low-speed (LS) test section, lateral force (a), rolling moment (b), vertical force (c) and lee-rail rolling moment (d) aerodynamic coefficients for upwind and upwind + downwind rows of windbreaks as a function of the yaw angle $\beta_{w.}$

655
656

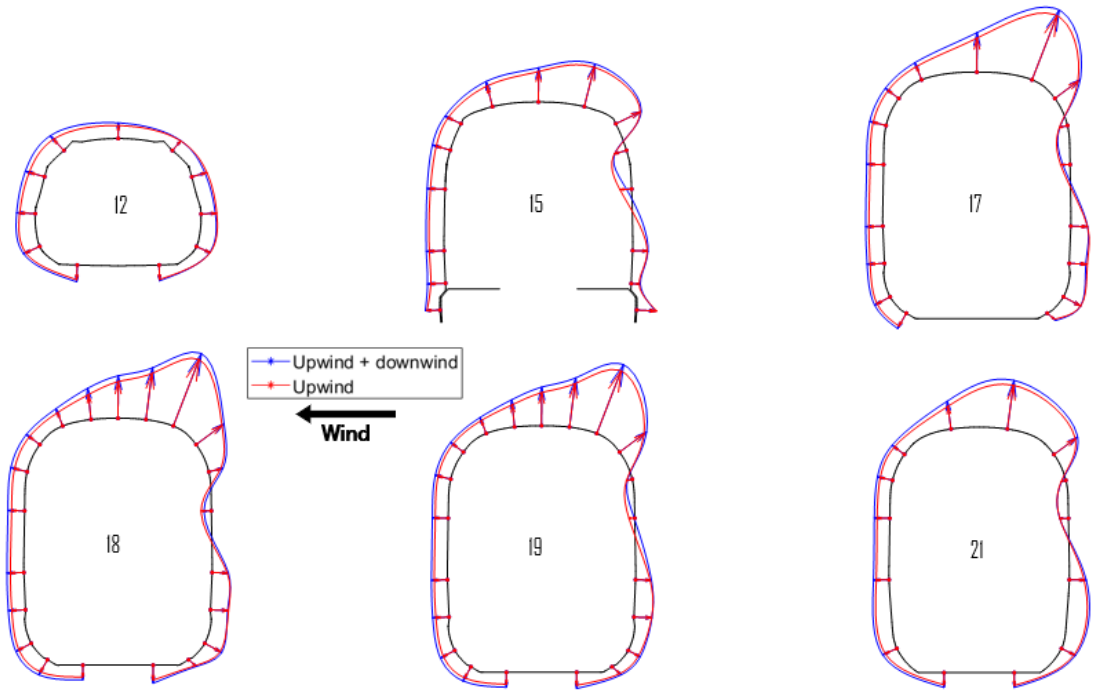

Figure 18: porous windbreaks (BP), low-speed (LS) test section, pressure coefficients for upwind and upwind + downwind rows of windbreaks and $\beta_w = 40°$

657
658

4 Conclusions

In this work, several wind tunnel tests on a high-speed train model were conducted with different windbreaks and scenario configurations: by comparing the results obtained in terms of force/moment coefficients and pressure coefficients, it was possible to evaluate the effects of different parameters (related to the flow and related to the flow and geometric characteristics) associated with these tests. Starting from the analysis of the results, guidelines to plan wind tunnel tests for trains with windbreaks are proposed, with final goal of obtaining aerodynamic results that are as representative as possible of the real full-scale condition.

The main findings of this study are summarised below.

1. The presence of porous or solid windbreaks significantly reduces the dependence on the *Re number*, especially at high yaw angles. The double behaviour of the flow, observed in the configurations without barriers and due to the combination of a train's smooth geometry and the Reynolds number, disappears in the tests with barriers. Moreover, as already found in previous papers [23], the increase in the *turbulence intensity* leads to a higher local Re number and the corresponding coefficients are equivalent to those found with greater Reynolds numbers.
   Furthermore, the presence of windbreaks, especially solid ones, significantly reduces the coefficients' dependence on the *boundary layer* height.

2. For tests with solid windbreaks, particular attention must be given to the *width of the splitter plate*, especially for yaw angles over to β_w=30°. In particular, in this case, it was demonstrated that an upwind splitter plate width equal to about 3.75*H (H being the vehicle height) is not sufficient to obtain results that are representative of the real conditions and the corresponding coefficients can be underestimated by more than 30%. The aerodynamic phenomenon of the separation bubble that influences the incident flow depends on the geometry and structure of the supporting table and on the height of the barriers; therefore a specific verification, done using CFD simulations, during the wind tunnel test design phase is recommended. On the other hand, for windbreaks with higher porosities a splitter plate 3.75*H wide is sufficient to correctly represent the incident flow.

3. For both solid and porous windbreaks, the *length of the barriers in front of the train* is fundamental and causes important differences in the aerodynamic coefficients especially at low yaw angles and can lead to erroneous conclusions on the crosswind safety of high-speed trains as well. For the case considered, a length of about 2.35*H was found to be insufficient to avoid overestimation of the coefficients by about 25% in the range β_w = 0° - 60° due to the reduction in the protection provided by the barrier and to the flow channelling effect.

4. Finally, coefficients measured with only the upwind row of barriers are lower (up to 50%), especially at high yaw angles, than those measured with the standard configuration with two rows of barriers (upwind + downwind). As a consequence, if the real setup is standard, both rows of windbreaks must be reproduced in the wind tunnel and the only upwind setup simplification is not allowed.

In conclusion, in order for wind tunnel tests to represent the real full-scale conditions of a train in presence of windbreaks as accurately as possible, it is necessary to pay attention to correctly control the flow parameters (Re number and turbulence intensity) and, especially, the scenario model (width of the splitter plate, length of the barriers in front of the train).

5 References

[1] Baker, C. J., *A review of train aerodynamics Part 1 – Fundamentals*. The Aeronautical Journal vol118, no.1201, 2014.

[2] Baker, C. J., *A framework for the consideration of the effects of crosswinds on trains*, Journal of Wind Engineering & Industrial Aerodynamics. 123(2013) 130–142, 2013.

[3] European Commission. *Technical specification for interoperability relating to the "rolling stock locomotives and passenger rolling stock" subsystem of the rail system in the European Union*. Official Journal of the European Union. 2014.

[4] EN14067. *Railway applications – Aerodynamics* –. 2006.

[5] Hemida, H., S. Krajnovic. *LES study of the influence of the nose shape and yaw angles on flow structures around trains*. Journal of Wind Engineering and Industrial Aerodynamics. 2010.

[6] Bocciolone, M., Cheli, F., Corradi, R., Muggiasca, S., G. Tomasini. *Crosswind action on rail vehicles: Wind tunnel experimental analyses*. Journal of Wind Engineering and Industrial Aerodynamics. 96 (2008), pp. 584-610 2008.

[7] Li, T., Zou, Y-S, Zhang, W-H. *Dynamic performance of high-speed train passing windbreak in crosswind*. J China Rail Soc. 2018.

[8] Liu, T., Chen, Z., Zhou, X., Zhang J. *A CFD analysis of the aerodynamics of a high-speed train passing through a windbreak transition under crosswind*. Engineering Applications of Computational Fluid Mechanics. 2018.

[9] Wang, D., Chen, D., Li, M., Liu, G. *Research on Aerodynamic Characteristic for EMU Passing by Windbreak Wall Gap under Crosswind*. Advances in Engineering Research. 2016.

[10] Sun, Z., Dai, h., Hemida, H., Li, T., Huang, C. *Safety of high-speed train passing by windbreak breach with different sizes*, Vehicle System Dynamics. 2019.

[11] Yang, W., Deng, E., Lei, M., Zhihui, Z., Zhang, P. *Transient aerodynamic performance of high-speed trains when passing through two windproof facilities under crosswinds: A comparative study*. Engineering Structures. 2019.

[12] Hashmi S.A., Hemida H., Soper D. *Wind tunnel testing on a train model subjected to crosswinds with different windbreak walls.* Journal of Wind Engineering & Industrial Aerodynamics 195 104013, 2019.

[13] F. Dorigatti, M. Sterling, C.J. Baker, A.D. Quinn. *Crosswind effects on the stability of a model passenger train—a comparison of static and moving experiments*. J. Wind Eng. Ind. Aerod., 138. 2015

[14] Agnieszka Kocoń, Andrzej Flaga, *Critical velocity measurements of freight railway vehicles roll-over in wind tunnel tests as the method to assess their safety at strong cross winds*, Journal of Wind Engineering and Industrial Aerodynamics, Volume 211, 2021, 104559, ISSN 0167-6105, https://doi.org/10.1016/j.jweia.2021.104559.

[15] Catanzaro, C., Cheli, F., Rocchi, D., Schito, P.,Tomasini, G. *High-speed train crosswind analysis: CFD study and validation with wind-tunnel tests*. Lecture Notes in Applied and Computational Mechanics. 2016.

[16] Telenta, M. & Šubelj, M. & Tavcar, Jo. & Duhovnik, J. Detached Eddy Simulation of the flow around a simplified vehicle sheltered by wind barrier in transient yaw crosswind. Mechanics. 21. 10.5755/j01.mech.21.3.8942. 2015.

[17] Tomasini, G., Giappino, S., Cheli, F., Schito P., *Windbreaks for railway lines: Wind tunnel experimental tests.* Proceedings of the Institution of Mechanical Engineers, Part F: Journal of Rail and Rapid Transit. 2015.

[18] Niu J., Zhou D., Wang Y. *Numerical comparison of aerodynamic performance of stationary and moving trains with or without windbreak wall under crosswind*. Journal of Wind Engineering & Industrial Aerodynamics 182. 2018

[19] A. Premoli, D. Rocchi, P. Schito, G. Tomasini. *Comparison between stationary and moving railway vehicles subjected to crosswind by CFD analysis*. J. Wind Eng. Ind. Aerod., 156. 2016.

[20] E. Brambilla, C. Araya, P. Schito, G. Tomasini. *Procedure for evaluating crosswind safety of a train running in presence of windbreaks with gap, part 1: determination of the aerodynamic loads* Fourth international conference in numerical and experimental aerodynamics of road vehicles and trains (Aerovehicles 4). 2021

[21] Zhang L., Yang M., Liang X*. Experimental study on the effect of wind angles on pressure distribution of train streamlined zone and train aerodynamic forces*. Journal of Wind Engineering and Industrial Aerodynamics, Volume 174. 2018.

[22] Yang Z., Igarashi H., Martin M., Hu H., *An Experimental Investigation on Aerodynamic Hysteresis of a Low-Reynolds Number Airfoil,* 6th AIAA Aerospace Sciences Meeting and Exhibit, Reno, Nevada 2008.

[23] F. Cheli, S. Giappino, L. Rosa, G. Tomasini, M. Villani, *Experimental study on the aerodynamic forces on railway vehicles in presence of turbulence*. Journal of Wind Engineering and Industrial Aerodynamics, Volume 123. 2013.